Arc-Faults Detection in PV Systems by Measuring Pink Noise With Magnetic Sensors

Wenchao Miao, Xuyang Liu, K. H. Lam, and Philip W. T. Pong

Department of Electrical and Electronic Engineering, The University of Hong Kong, Hong Kong

The dc-arc detection is essential for dc systems to operate reliably and safely. Due to the randomness of dc-arc faults, it is difficult to define their characteristics for detection. The magnetic-sensing-based methodology using tunnel magnetoresistance (TMR) sensor was developed to distinguish the dc arc accurately. However, the noise from the power electronics such as maximum power pointing tracking (MPPT) controllers could affect the dc-arc detection in a photovoltaic (PV) system. In this paper, the arc faults which may occur in PV systems under various conditions were emulated in the dc system of 9 kW. It was verified that the proposed methodology of measuring pink noise can distinguish the dc arc accurately for PV systems from 48 to 300 V and current up to 30 A. An off-grid PV system was established to experimentally demonstrate the arc-detection method in the practical system. The experimental results confirmed that the technique could identify the dc arc correctly with an extended working region despite the noise of power electronics in MPPT. It was verified that the arc-detection system is capable of discriminating the normal operation and arc fault in the PV system. This technique is applicable and promising for arc-faults detection in PV systems.

Index Terms—**Direct current (dc) arc fault, fault detection, magnetoresistive sensor, photovoltaic (PV) system.**

I. Introduction

DIRECT current (dc) arc faults occur accidentally due to the failure of the intended continuity of a conductor or connector in the dc systems. The undetected arc faults challenge the reliability, efficiency, and safety of the dc system since they may cause malfunctions and even lead to fire hazards [1]. To prevent the electric arc hazards, National Electrical Code specifies that arc-fault protection is mandatory for photovoltaic (PV) systems with a maximum voltage larger than 80 V [2]. However, the complexities and randomness of dc-arc faults aggravate the difficulty of defining their characteristics for detection [3], [4]. Though various dc-arc-detection techniques based on wavelet transformation, electromagnetic radiation or frequency-spectrum analysis have been widely researched [4]–[6], they have limitations as summarized in [7]. There are also techniques based on the time-domain analysis which directly adopt the time-domain signatures of dc arc for detection [8], [9]. However, it is difficult to prevent nuisance tripping from other faults. Thus, reliable techniques to detect arc are still lacking.

Furthermore, these techniques have not been fully examined under experimental conditions and assessed in practical dc systems. The characteristics of dc arc were studied at different power ratings with a simplified experimental setup, but the proposed detection methodology has not been examined at the system level [4]. Although PV panels were used as a power source in [10], a PV system was not developed to examine the detection technique. An arc detector was designed to identify arcing in PV systems [4], [11], [12], but it suffers from nuisance tripping caused by the inverter or other power electronics in the system [13]. The characteristics of dc arc vary with the power level and gap length [4], [14], [15], and the accuracy of the detection techniques, when applied in PV systems, is not guaranteed [6], [11]. Therefore, it is essential to investigate the dc arc under various experimental conditions to develop a reliable dc-arc-detection technique and examine the technique in the PV systems.

Previously, we developed a promising magnetic-sensing-based technique using the cost-effective and compact tunnel magnetoresistance (TMR) sensor to detect arc in [7]. The characteristics of dc arc in the frequency domain were defined. The pink noise was shown to be generated by arcing. The parameters, which can clearly distinguish the dc arc, were derived from the analysis of the pink noise. However, the voltage, current, and gap length vary with the dc systems and they may affect the arc-faults detection.

First, the gap lengths of series arc faults in PV systems are arbitrary. Thus, the effect of gap length on frequency spectra requires further study for PV systems [14], [15]. Second, the frequency-domain characteristics of arcing can be affected by the power level of PV systems [15]. It is necessary to extend the voltage and current ranges of the proposed method for detecting arcing in PV systems. Third, the noise from the power electronics in PV systems can affect the arc-faults detection [13]. Therefore, it is essential to overcome these new challenges to further develop and refine the arc-detection technique for PV systems.

In this paper, a dc system was used to emulate the possible series arc-faults in PV systems. Since 48 V is commonly adopted in the battery bank of PV systems [16], [17] and their dc bus is usually several hundred volts [18], [19], the experiments in the dc system were conducted from 48 to 300 V and current up to 30 A. An off-grid PV system was developed to experimentally demonstrate the performance of the technique. A widely used 48 V battery system was adopted in the

Manuscript received November 5, 2018; revised February 21, 2019; accepted March 6, 2019. Corresponding author: P. W. T. Pong (e-mail: ppong@eee.hku.hk).

Color versions of one or more of the figures in this paper are available online at http://ieeexplore.ieee.org.

Digital Object Identifier 10.1109/TMAG.2019.2903899

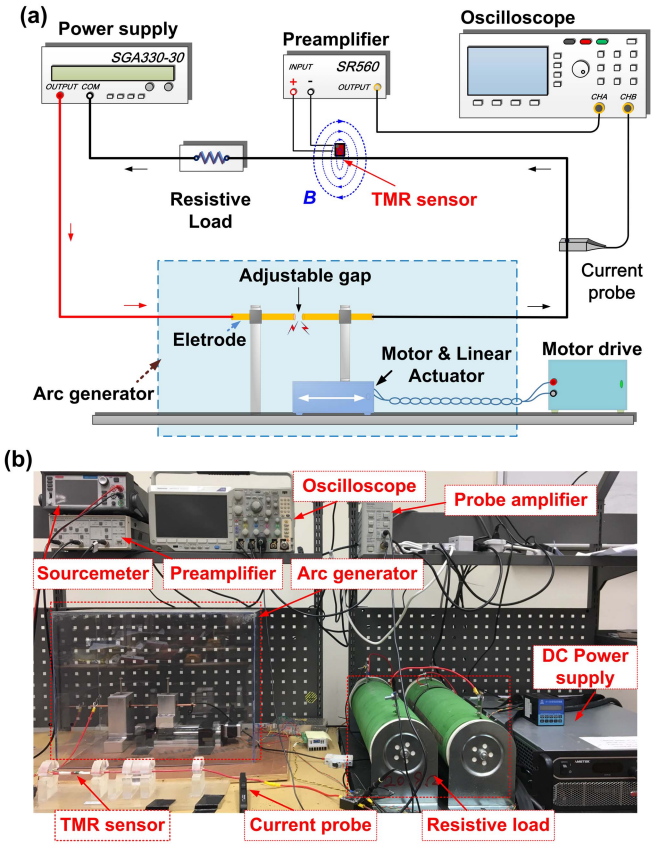

Fig. 1. Experimental setup for emulation of dc arc in PV systems. (a) Schematic of the setup. (b) Photograph of the setup.

PV system to test the arc-detection technique in the general condition as a demonstration.

In Section II, the experimental setup and the arc-detection methodology to distinguish the normal operation and sustained arcing is presented. In Section III, the capability of the arc-detection methodology for PV systems was verified in various conditions of gap length, voltage, and current. The applicability of the arc-detection technique in a PV system installed with power electronics was tested and verified. The conclusion is drawn in Section IV.

II. Experimental Setup and Detection Methodology

The diagram and photograph of the experimental setup to emulate the series dc-arc in PV systems are shown in Fig. 1 (a) and (b), respectively. The TMR sensor (TMR2001, MultiDimension) [20] and current probe were capable of measuring the load current in normal operation and sustained arcing as demonstrated in [7]. The experimental conditions emulating typical PV systems are displayed in Table I. The effect of gap length was investigated from 0.4 to 1 mm.

Since the frequency spectrum of the load current is composed of both pink and white noises when the arc fault occurs [7], [21], [22], the pink noise equation (1) was applied to fit the frequency spectra of the current in normal operation and sustained arcing [7]. Then, the presence of the dc arc can be determined by the combined parameters derived by using the fitting results [7]. The difference between normal operation and sustained arcing in decibels can be calculated

$$S(f) = \frac{A}{f^{\gamma}} + c \tag{1}$$

where S is the power spectral density (PSD), f is the frequency, and A, γ, and c are constants.

TABLE I
Experimental Conditions

Electrode Material	Copper
Electrode Diameter (mm)	3
Gap Length (mm)	0.4, 0.6, 0.8, 1
Supply Voltage (V)	48 to 300 in step of 36
Load Current (A)	6 to 30 in step of 6

III. Arc-Fault Detection in PV Systems

A. Gap-Length Effects on Arcing

The arc faults may happen at different gap lengths, and the characteristics of arcing differ with the gap length in PV systems [14], [15]. The frequency spectra of the arc current vary with the gap length [15]. Thus, it is important to ensure that the detection technique can effectively detect the arc faults at different gap lengths in PV systems. To study the effect of gap length on arcing, experiments were carried out at 48 and 120 V with the electrode diameter of 3 mm and supplied with 6 A. The gap length of 0.4, 0.6, 0.8, and 1 mm was tested. The gap of 1 mm was too large to induce the dc arc at 48 V. Therefore, only the frequency spectra of normal operation and sustained arcing in 0.4, 0.6, and 0.8 mm at 48 V were reported, as shown in Fig. 2(a).

When the system was in normal operation, no arcing was generated with a gap length less than 0.4 mm at 48 and 120 V. According to Fig. 2(a) and (b), the PSD of sustained arcing increased with the gap length and this phenomenon appeared at both 48 and 120 V. Therefore, it can be summarized that the pink noise generated by arcing increased with the gap length. Though the PSD of sustained arcing was relatively low at 0.4 mm, the difference between normal operation and sustained arcing was still obvious at both 48 and 120 V.

B. Emulation of the DC Arc in PV Systems

The arc-faults detection technique is based on the frequency-domain signatures of arcing. However, the frequency-domain characteristics of arcing can be affected by the power level of PV systems [15]. The dc arc in PV systems was emulated with the electrode diameter of 3 mm and a gap length of 0.6 mm by using the setup in Fig. 1. The voltage from 48 to 300 V with the current increased from 6 to 30 A was studied. Since the effect of electrode diameter on arcing was insignificant [7], only the electrode diameter of 3 mm was implemented. The gap length of 0.6 mm was used because it can induce dc arc through the whole voltage and current range. The frequency spectra of the load current were fit by (1). The fitting results of slope (γ) and magnitude (A) at 6 A are shown in Fig. 3(a) and (b) as an example. The parameter differences of the fitting results of

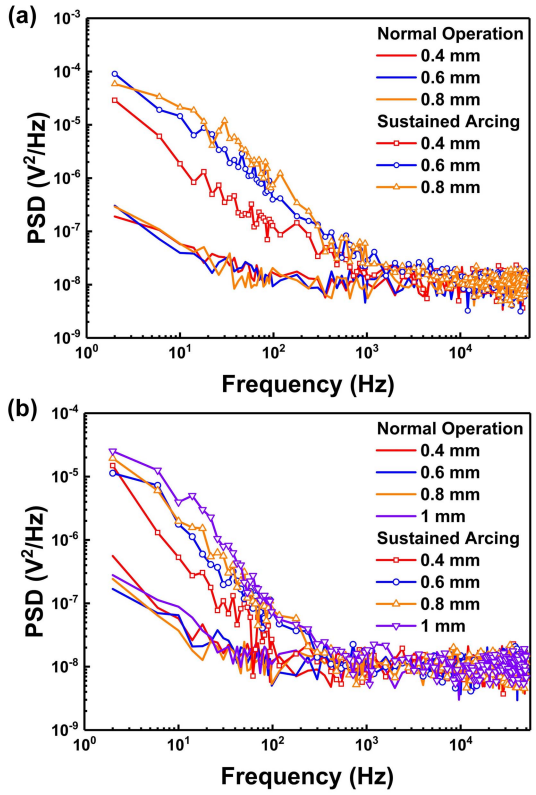

Fig. 2. Frequency spectra of the current at 6 A with the gap length of 0.4, 0.6, 0.8, and 1 mm when supplied with (a) 48 and (b) 120 V.

γ and A between normal operation and sustained arcing can be applied to identify arcing as explained in [7]. Similarly, the combined parameter P was derived from γ and A using (2) to distinguish the normal operation and sustained arcing.

The results of A and combined parameter P in Fig. 3(b) and (c) are much larger than the previous results in [7]. According to (2), the combined parameter P increases with A. Due to the experimental environment and the equipment condition, the white noise was larger than before in [7], causing the increment of A and combined parameter P. Nevertheless, the combined parameter P can be applied to identify dc arc since it showed a clear discrepancy between normal operation (P_{i-N}) and sustained arcing (P_{i-S}) throughout the whole voltage range from 48 to 300 V and current range from 6 to 30 A as depicted in Fig. 3(c). The difference between P_{i-S} and P_{i-N} in decibels was calculated using (3), and the minimum difference was 16.6 dB as shown in Fig. 3(d), which was consistent with the results in [7]. Since both the P_{i-N} and P_{i-S} were dependent on the white noise, they were enlarged with the same magnification. Therefore, similar differences in decibels were achieved.

In summary, the arc-fault detection technique was capable of detecting dc arc under various situations of gap length throughout the voltage range from 48 to 300 V and current up to 30 A.

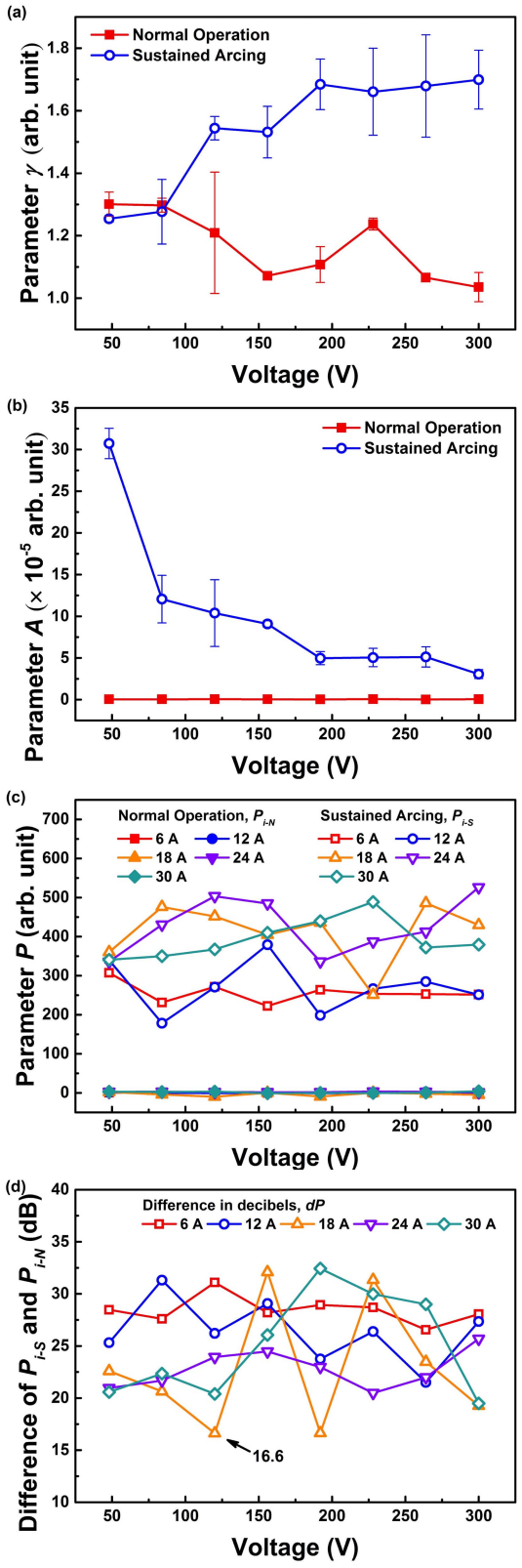

Fig. 3. Fitting results of normal operation and sustained arcing from 48 to 300 V. Fitting results of (a) γ and (b) A at 6 A. (c) Combined parameter P at 6, 12, 18, 24, and 30 A. (d) Difference between P_{i-S} and P_{i-N} in decibels.

C. Experimental Demonstration in Off-Grid PV System

Since the current arc-detection techniques may suffer from the nuisance tripping caused by the power electronics [4], [11]–[13], it is necessary to test the technique in a practical system. The performance of the arc-detection technique based on pink-noise measurement was studied in the off-grid PV

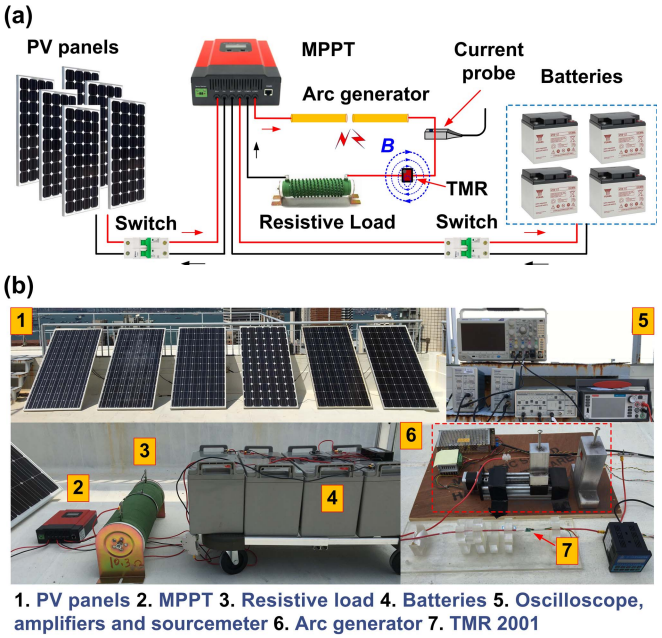

Fig. 4. Off-grid PV system with a series-connected arc generator. (a) Schematic and (b) photographs of the PV system.

system to verify its capability in a practical system. An off-grid PV system consisting of PV panels, switches, maximum power pointing tracking (MPPT) charge controller and batteries was developed, as shown in Fig. 4. It is well-known that the power electronics in the MPPT could introduce noise to the system [4], [11]. The six PV modules (JW-G1900, Jiawei Solarchina) in 190 W with a maximum operating voltage of 38.1 V were used. They were series connected in three strings with two panels per string and then parallel connected to obtain an output voltage of 76.2 V. Four lead-acid batteries, each 12 V 100 Ah, were series connected as the energy storage. The arc generator was series connected between the resistive load and MPPT to generate the series arc faults [23]. The batteries supplied the resistive load through the MPPT. Similarly, the TMR sensor and current probe were used to measure the current in normal operation and sustained arcing.

The technique was tested under a general condition with the arc faults occurred on the battery side. The experiments were carried out with the electrode diameter in 3 mm and a gap length of 0.6 mm. The arc generator, resistive load, and MPPT were series connected as shown in Fig. 4(a). The PV panels were charging the batteries through the MPPT. The batteries were working as a supply of 48.98 V to the resistive load with the current of around 4.76 A in normal operation as measured by TMR2001 in Fig. 4(a). The frequency spectra of the current in normal operation and sustained arcing as shown in Fig. 5(c) were extracted from a period of 0.5 s of their time-domain current waveforms in Fig. 5(a). It could be seen that there was a significant increase in the PSD which was in agreement with the results attained with the dc power supply.

The arc-fault detection techniques based on frequency-spectra analysis are suffering from the nuisance tripping caused by the power electronics noise in PV systems [13]. To detect the dc arc, the predefined threshold of an arc-fault

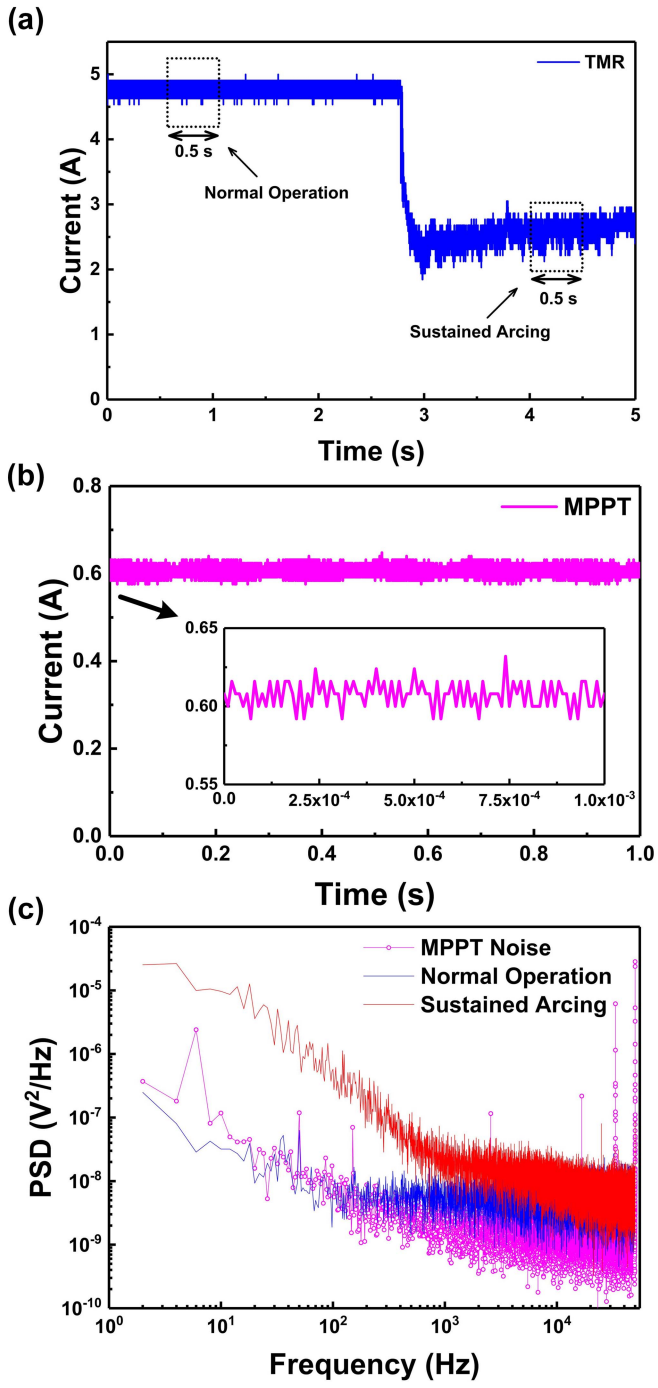

Fig. 5. Arc current when supplied with batteries and MPPT. The time domain of (a) arc current, (b) current through MPPT, and (c) frequency spectra of the current.

detector must be lower than or equal the PSD of sustained arcing. However, the frequency spectra of the noise caused by the power electronics may reach the predefined threshold leading to nuisance tripping. The current through the MPPT was measured by the conventional current probe, as shown in Fig. 5(b). The current contained the power electronic noise due to the MPPT. There was a large increment of PSD at the frequency lower than 20 Hz and from 30 to 50 kHz, as shown in Fig. 5(c) due to the MPPT. By using the pink-noise analysis, the combined parameter P shows

TABLE II
FITTING RESULTS OF THE FREQUENCY SPECTRA

Parameter	Noise	Normal Operation	Sustained Arcing
γ	0.95126	1.07024	1.26502
A	8.19166×10^{-7}	5.31529×10^{-7}	1.24417×10^{-4}
P	0.819043	0.53182	124.41765
dP (dB)	21.82	23.69114	

TABLE III
CURRENT SENSORS USED IN DC-ARC DETECTION

Sensor	Manufacturer	Bandwidth (MHz)	Size (cm)	Cost (USD)
Current Probe	Tektronix, TCP 300A [4]	100	20.0*6.0*3.2	~1,720
Current Transformer	Ion Physics, CM-1-L [15]	10	11.8*10.2*3.0	~200
	Pearson, 110A [24]	20	11.2*10.2*2.5	~595
Hall Sensor	LA55-P/SP50 [25]	0.2	3.7*2.7*1.4	~37.53
GMR sensor	AA002-02 [26]	1	0.62 *0.5*0.4	~13.85
TMR Sensor	MultiDimension, TMR2001 [20]	1	0.3*0.3*0.15	~2.54

a clear discrepancy of 21.82 dB between the frequency spectra of the MPPT noise and the sustained arcing, as provided in Table II. An apparent difference of approximately 23.69 dB between normal operation and sustained arcing was achieved. The technique was capable of detecting the dc arc of the off-grid PV system in this circumstance. The arc-faults detection technique was not vulnerable to the noise of power electronics in MPPT. Therefore, the power electronic noise from MPPT was not affecting the accuracy of the proposed arc-detection methodology based on pink-noise analysis.

Although other current sensors such as current probes and current transformers (CTs) or magnetic sensors such as hall sensors and giant magnetoresistance (GMR) sensors can be used to implement the proposed arc-detection technique by measuring pink noise, they suffer from various drawbacks. The size and approximate cost of sensors used in other researches are summarized in Table III. The current probes and CTs are bulky and expensive, and CTs can only measure the alternating current. The hall sensors are relatively small with the lower expense, but the bandwidth is limited. The information about TMR2001 and GMR AA002-02 are also included. Generally, the sensitivity of GMR is lower than TMR. The sensitivity of GMR AA002-02 of 4.2 mV/V/Oe is much lower than the TMR2001 with the sensitivity of 8 mV/V/Oe. And, the price of AA002-02 is higher. The compact TMR sensor is cost-effective and can be widely implemented in power systems for arc-fault detection. It is non-contact, and it does not require making contact or clamping around the cable. It provides a convenient and low-cost methodology for PV power plants especially when arc-fault detection in a large number of PV arrays are required.

IV. CONCLUSION

The dc arc-faults detection technique based on pink-noise measurement by magnetic sensors was capable of detecting dc arc under the voltage from 48 to 300 V, current from 6 to 30 A, and the minimum gap length of 0.4 mm with the experimental setup. The technique was further demonstrated in the off-grid PV system. The results showed that the technique could still effectively detect series arcing under the influence of the power electronics in MPPT. In this paper, the dc arc was only examined on the load side at a single voltage and current level. The applicability and accuracy of the arc-detection system will be further investigated in different configurations of the PV system in the future. The effects of the location of dc arc, the voltage, and current levels will also be studied.

ACKNOWLEDGMENT

This work was supported in part by the Seed Funding Program for Basic Research, in part by the Seed Funding Program for Applied Research, in part by the Small Project Funding Program from The University of Hong Kong, Hong Kong, in part by the ITF Tier 3 Funding under Grant ITS/203/14, Grant ITS/104/13, and Grant ITS/214/14, in part by RGC-GRF under Grant HKU 17204617, and in part by the University Grants Committee of Hong Kong under Contract AoE/P-04/08.

REFERENCES

[1] M. K. Alam, F. Khan, J. Johnson, and J. Flicker, "A comprehensive review of catastrophic faults in PV arrays: Types, detection, and mitigation techniques," *IEEE J. Photovolt.*, vol. 5, no. 3, pp. 982–997, May 2015.

[2] *National Electrical Code 2014 Handbook*, 13th ed., Nat. Fire Protection Assoc., Quincy, MA, USA, 2013.

[3] R. F. Ammerman, T. Gammon, P. K. Sen, and J. P. Nelson, "DC-arc models and incident-energy calculations," *IEEE Trans. Ind. Appl.*, vol. 46, no. 5, pp. 1810–1819, Sep./Oct. 2010.

[4] X. Yao, L. Herrera, S. Ji, K. Zou, and J. Wang, "Characteristic study and time-domain discrete-wavelet-transform based hybrid detection of series DC arc faults," *IEEE Trans. Power Electron.*, vol. 29, no. 6, pp. 3103–3115, Jun. 2014.

[5] C. J. Kim, "Electromagnetic radiation behavior of low-voltage arcing fault," *IEEE Trans. Power Del.*, vol. 24, no. 1, pp. 416–423, Jan. 2009.

[6] Texas Instruments, Dallas, TX, USA. (2012). *AN-2154 RD-195 DC Arc Detection Evaluation Board*. Accessed: Nov. 3, 2018. [Online]. Available: http://www.ti.com/lit/ug/snoa564f/snoa564f.pdf

[7] W. Miao, X. Liu, K. H. Lam, and P. W. T. Pong, "DC-arcing detection by noise measurement with magnetic sensing by TMR sensors," *IEEE Trans. Magn.*, vol. 54, no. 99, Nov. 2018, Art. no. 4002005.

[8] M. Naidu, T. J. Schoepf, and S. Gopalakrishnan, "Arc fault detection scheme for 42-V automotive DC networks using current shunt," *IEEE Trans. Power Electron.*, vol. 21, no. 3, pp. 633–639, May 2006.

[9] S. Chen, X. Li, and J. Xiong, "Series arc fault identification for photovoltaic system based on time-domain and time-frequency-domain analysis," *IEEE J. Photovolt.*, vol. 7, no. 4, pp. 1105–1114, Jul. 2017.

[10] Z. Wang and R. S. Balog, "Arc fault and flash signal analysis in DC distribution systems using wavelet transformation," *IEEE Trans. Smart Grid*, vol. 6, no. 4, pp. 1955–1963, Jul. 2015.

[11] S. McCalmont, "Low cost arc fault detection and protection for PV systems: January 30, 2012–September 30, 2013," Nat. Renew. Energy Lab., Golden, CO, USA, Tech. Rep. NREL/SR-5200-60660, Sep. 2013.

[12] J. Johnson and J. Kang, "Arc-fault detector algorithm evaluation method utilizing prerecorded arcing signatures," in *Proc. 38th IEEE Photovolt. Spec. Conf.*, Jun. 2012, pp. 1378–1382.

[13] J. Johnson, C. Oberhauser, M. Montoya, A. Fresquez, S. Gonzalez, and A. Patel, "Crosstalk nuisance trip testing of photovoltaic DC arc-fault detectors," in *Proc. 38th IEEE Photovolt. Spec. Conf.*, Jun. 2012, pp. 1383–1387.

[14] F. M. Uriarte *et al.*, "A DC arc model for series faults in low voltage microgrids," *IEEE Trans. Smart Grid*, vol. 3, no. 4, pp. 2063–2070, Dec. 2012.

[15] M. Wendl, M. Weiss, and F. Berger, "HF characterization of low current DC arcs at alterable conditions," in *Proc. 27th Int. Conf. Electr. Contacts (ICEC)*, Jun. 2014, pp. 1–6.

[16] E. Rodriguez-Diaz, F. Chen, J. C. Vasquez, J. M. Guerrero, R. Burgos, and D. Boroyevich, "Voltage-level selection of future two-level LVDC distribution grids: A compromise between grid compatibiliy, safety, and efficiency," *IEEE Electrific. Mag.*, vol. 4, no. 2, pp. 20–28, Jun. 2016.

[17] S. Anand and B. G. Fernandes, "Optimal voltage level for DC microgrids," in *Proc. IEEE 36th Annu. Conf. Ind. Electron. Soc.*, Nov. 2010, pp. 3034–3039.

[18] S. Kouro, J. I. Leon, D. Vinnikov, and L. G. Franquelo, "Grid-connected photovoltaic systems: An overview of recent research and emerging PV converter technology," *IEEE Ind. Electron. Mag.*, vol. 9, no. 1, pp. 47–61, Mar. 2015.

[19] D. Salomonsson and A. Sannino, "Low-voltage DC distribution system for commercial power systems with sensitive electronic loads," *IEEE Trans. Power Del.*, vol. 22, no. 3, pp. 1620–1627, Jul. 2007.

[20] MultiDimension. *TMR2001*. Accessed: Feb. 21, 2019. [Online]. Available: http://www.dowaytech.com/en/index.php?c=download&id=2025

[21] J. Keenan and M. Parker, "Arc detectors," in *Proc. 20th Int. Telecommun. Energy Conf. (INTELEC)*, Oct. 1998, pp. 710–715.

[22] J. Johnson *et al.*, "Photovoltaic DC arc fault detector testing at sandia national laboratories," in *Proc. 37th IEEE Photovolt. Spec. Conf.*, Jun. 2011, pp. 3614–3619.

[23] Q. Xiong, S. Ji, L. Zhu, L. Zhong, and Y. Liu, "A novel DC arc fault detection method based on electromagnetic radiation signal," *IEEE Trans. Plasma Sci.*, vol. 45, no. 3, pp. 472–478, Mar. 2017.

[24] J. Johnson *et al.*, "Differentiating series and parallel photovoltaic arc-faults," in *Proc. 38th IEEE Photovolt. Spec. Conf.*, Jun. 2012, pp. 720–726.

[25] L. Yuan, J. Shengchang, W. Jin, Y. Xiu, and Z. Yeye, "Study on characteristics and detection of DC arc fault in power electronics system," in *Proc. Int. Conf. Condition Monitor. Diagnosis*, Sep. 2012, pp. 1043–1046.

[26] NVE Corporation. *AA002-02*. Accessed: Feb. 21, 2019. [Online]. Available: https://www.km-cs.com/dir/nve/aa002.pdf